JOC The Journal of Organic Chemistry

Article

pubs.acs.org/joc

Aminobenzofuran-Fused Rhodamine Dyes with Deep-Red to Near-Infrared Emission for Biological Applications

Guangle Niu,[†,‡] Weimin Liu,[*,†] Jiasheng Wu,[†] Bingjiang Zhou,[†,‡] Jianhong Chen,[†,‡] Hongyan Zhang,[†] Jiechao Ge,[†] Ying Wang,[†] Haitao Xu,[†] and Pengfei Wang[†]

[†]Key Laboratory of Photochemical Conversion and Optoelectronic Materials and CityU-CAS Joint Laboratory of Functional Materials and Devices, Technical Institute of Physics and Chemistry, Chinese Academy of Sciences, Beijing 100190, China

[‡]University of Chinese Academy of Sciences, Beijing 100049, China

Supporting Information

ABSTRACT: Aminobenzofuran-fused rhodamine dyes (**AFR** dyes) containing an amino group were constructed by an efficient condensation based on 3-coumaranone derivatives. **AFR** dyes exhibited significantly improved properties, including deep-red and near-infrared emissions, a large Stokes shift, good photostability, and wide pH stability. 3-(4,5-Dimethylthiazol-2-yl)-2,5-diphenyl-2*H*-tetrazolium assay experiments show that these **AFR** dyes are biocompatible for their low cytotoxicity to both A549 and HeLa cells. Cell imaging data reveal that **AFR1**, **AFR1E**, and **AFR2** are mainly located in the mitochondria, while **AFR3** is a lysosome tracker. As far as we know, NIR **AFR3** is the longest fluorescent rhodamine derivative containing the amino group. These amino group-containing **AFR** dyes hold great potential in fluorogenic detection, biomolecule labeling, and cell imaging.

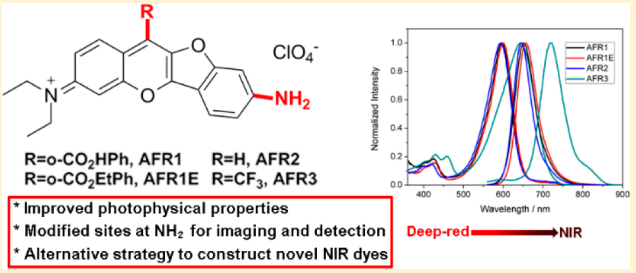

INTRODUCTION

Compared with other generally used dyes, rhodamine derivatives have received considerable attention in biomolecule labeling and detection, cancer diagnosis, and other biological applications because of their outstanding photophysical properties, such as high molar extinction coefficients, large fluorescence quantum yields, and resistance to photobleaching.[1] In addition, chemical modification of rhodamine dyes is a straightforward process.[2] For example, modification of the amino group on the ring of the rhodamine moieties is usually utilized to detect cancer-related markers or significant biomolecules in living samples.[3] However, most rhodamine derivatives emit green to orange fluorescence. As we know, in contrast to short wavelength fluorophores, deep-red and near-infrared (NIR) dyes is advantageous to biodetection or imaging because of the minimal photodamage to biological samples, deep tissue penetration, and minimal interference from background autofluorescence in living systems.[4]

Substantial efforts have been made to synthesize rhodamine derivatives with longer emission wavelengths. The innovative work of replacing the bridged oxygen atom with other elements (Si, Ge, Sn, or Te) was proposed by Qian and Nagano et al.[5] An amino group-containing rhodamine dye with red emission (2Me SiR600; λ_{max} = 613 nm) was obtained by the Nagano group.[6] In addition, Abe's group synthesized a deep-red naphthyl-fused rhodamine derivative with an amino group (λ_{max} = 650 nm).[7] After that, a series of deep-red to NIR rhodamine derivatives were developed by extending the π-conjugation of the rhodamine skeleton by benzene or heteroaromatic rings.[8] Aside from the strategies mentioned above, introducing electron-withdrawing groups (CF_3 and CN) into the rhodamine skeleton at position 9 can also be utilized to increase the fluorescence wavelength of rhodamine dyes.[9] Just recently, another strategy was explored to obtain NIR rhodamine analogues by introducing phenylethynyl at position 9.[10] However, these strategies have some drawbacks, such as low production yield, tedious and rigorous synthesis, pH sensitivity, and a small Stokes shift.

Aromatic ring-fused dyes have high fluorescence quantum yields, good photostability, and longer emission wavelengths.[11] However, very few aromatic ring-fused rhodamine derivatives have been constructed, especially heteroaromatic rings.[7,8] Recently, our group synthesized a series of coumarin-fused rhodamine dyes (**CR** series) as a novel ratiometric detection platform, which exhibited deep-red emission, good fluorescence quantum yields, excellent photostability and low cytotoxity.[8b] In the study presented here, we design and synthesize another novel family of deep-red and NIR rhodamine derivatives (**AFR1**, **AFR1E**, **AFR2**, and **AFR3**) bearing an amino group by introducing benzofuran into the rhodamine skeleton (Scheme 1). These novel aminobenzofuran-fused rhodamine dyes have the advantage of a larger Stokes shift, longer emission wavelengths, and higher pH stability compared to those of the traditional rhodamine dyes. Cell cytotoxicity experiments reveal that these **AFR** dyes are biocompatible with both A549

Received: January 12, 2015
Published: February 18, 2015

ACS Publications © 2015 American Chemical Society

DOI: 10.1021/acs.joc.5b00077
J. Org. Chem. 2015, 80, 3170−3175

Scheme 1. Synthesis of Deep-Red and NIR Dyes AFR1, AFR1E, AFR2, and AFR3[a]

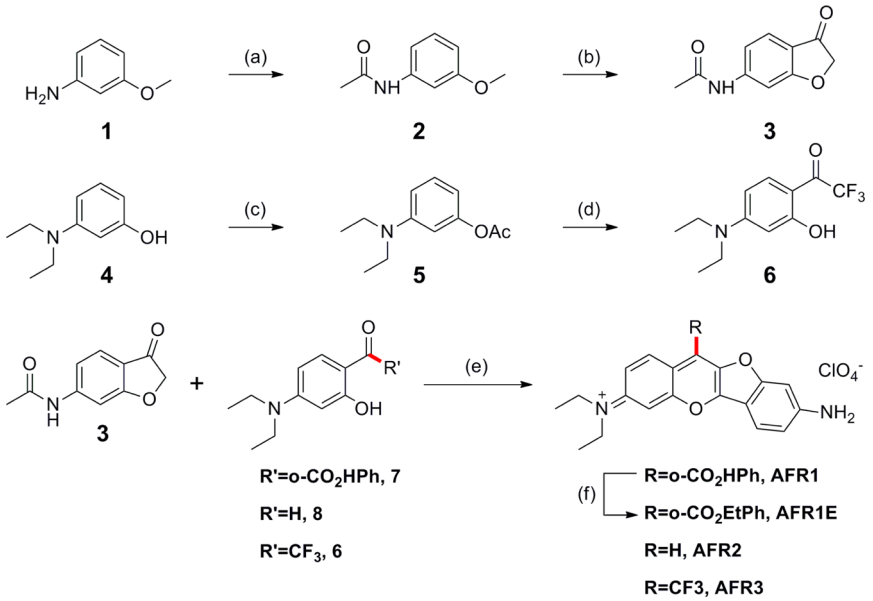

[a]Conditions: (a) Ac_2O, AcOH, 0 °C to rt, 24 h; (b) (1) $ClCH_2COCl$, $AlCl_3$, 1,2-dichloroethane, 0 °C to rt, 24 h; (2) AcONa, EtOH, reflux, 24 h; (c) Ac_2O, NEt_3, DMAP, rt, 12 h; (d) (1) TFAA, Et_2O, reflux, 3 h; (2) 2 N HCl, THF, rt, 24 h; (e) concentrated H_2SO_4, 100 °C, 4−8 h; (f) EtOH, concentrated H_2SO_4, reflux, 4 h.

and HeLa cells. The good photophysical properties of **AFR** dyes and the amino group contained in the rhodamine skeleton identify them as promising candidates for imaging-related biological applications.

RESULTS AND DISCUSSION

Design and Synthesis. The synthetic routes of the **AFR** dyes are outlined in Scheme 1. The key intermediate **3** was prepared using a previously published method.[12] First, the starting material **1** was protected by the acetyl group to obtain **2**. 2-Chloroacetyl chloride was the introduced into compound **2** via the Friedel−Crafts reaction. After cyclization reaction with AcONa in ethanol, the synthetic precursor **3** was obtained. Condensation of **3** and **7** in the presence of heated concentrated H_2SO_4 leads to **AFR1** with an excellent yield (90%), during which the acetyl group was automatically removed without further treatment. Likewise, **AFR2** was also synthesized by condensation of **3** and **8** with a high yield (69%). **AFR1E** was obtained from **AFR1** in ethanol catalyzed by concentrated H_2SO_4.

The introduction of electron-withdrawing groups such as CF_3 at position 9 of xanthenes leads to dyes with longer absorption and emission wavelengths.[9] The CF_3 group is introduced into the xanthene skeleton usually through a reaction between 3-alkylaminophenol and trifluoroacetic anhydride (TFAA). However, the production yield is low, and further conjugation is restricted because of the absence of functional groups.[9] Recently, Cornish proposed a new strategy by using the reaction of TFAA with a diaryl ether derivative with good yield.[13] Thus, a similar synthetic method was employed to synthesize **AFR3** by the reaction of **3** and **6** with a yield of 11%. The intermediate **6** was synthesized in three steps from the starting material **4**. Compound **5** that was prepared by acetylation of **4** reacted with TFAA via the Friedel−Crafts reaction and then was deacetylated by HCl in THF leading to **6**.[14] The final structures of **AFR** dyes were characterized via ^1H and ^{13}C NMR spectroscopy, HR-ESI, and element analysis.

Photophysics. The absorption and fluorescence data for **AFR1**, **AFR1E**, **AFR2**, and **AFR3** in distinct solvents (CH_2Cl_2, EtOH, and H_2O) are summarized in Table 1. Their corresponding spectra are shown in Figure 1 and Figures S1 and S2 of the Supporting Information. The maximal emission wavelengths (λ_{em}^{max}) of **AFR1**, **AFR1E**, and **AFR2** gradually increased from CH_2Cl_2 to EtOH to H_2O, which indicates the phenomenon of positive solvatochromism. Likewise, **AFR3** showed the same changing trend for emission in these solvents. As expected, **AFR3** emits NIR fluorescence because of the introduction of the electron-withdrawing group (CF_3) into the skeleton leading to a lower energy gap.[9] **AFR3** is the longest fluorescent rhodamine derivative containing an amino group. **AFR1**, **AFR1E**, and **AFR2** had good quantum yields in CH_2Cl_2 and EtOH, whereas the quantum yield of **AFR3** was

Table 1. Photophysical Properties of AFR Dyes in Different Solvents

dye	solvent	λ_{abs}^{max} (nm)	λ_{em}^{max} (nm)	Stokes shift (nm)	ε (M^{-1} cm^{-1})	Φ
AFR1	CH_2Cl_2	581	617	36	44400	0.726
	EtOH	572	622	50	113400	0.778
	H_2O	581	634	53	71400	0.126
AFR1E	CH_2Cl_2	587	627	40	74200	0.732
	EtOH	590	640	50	133200	0.501
	H_2O	588	645	57	86800	0.088
AFR2	CH_2Cl_2	597	623	26	89400	0.717
	EtOH	588	629	41	78800	0.584
	H_2O	583	627	44	94400	0.152
AFR3	CH_2Cl_2	658	695	37	92875	0.157
	EtOH	640	706	66	13880	0.064
	H_2O	640	707	67	36650	0.014

DOI: 10.1021/acs.joc.5b00077
J. Org. Chem. 2015, 80, 3170−3175

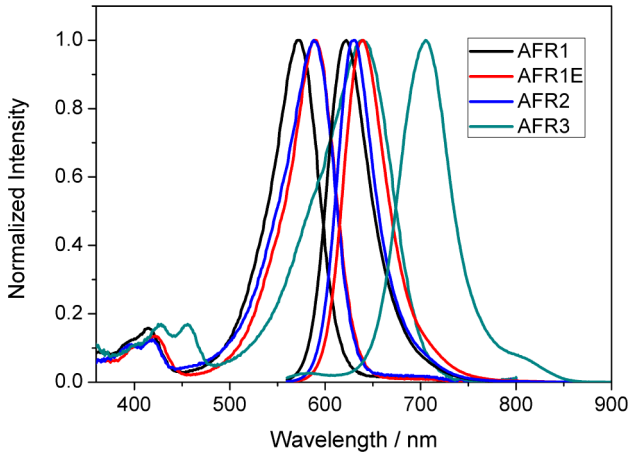

Figure 1. Normalized absorption and fluorescence spectra of **AFR** dyes in EtOH.

significantly reduced because of the decreased energy gap and enhanced nonradiative transition in NIR fluorescent dyes.[7,15] For the absorption wavelength (λ_{abs}^{max}) of **AFR** dyes in different solvents, no distinct regularity was observed except in the visible light and deep-red region (Figure 1). **AFR3** may be an excellent imaging dye because of excitation at the deep-red wavelength (640 nm), which largely reduced the level of photodamage and autofluorescence in living samples. The molar extinction coefficients of the **AFR** dyes ranged from 70000 to 134000 M^{-1} cm^{-1}, whereas few were in the region from 13000 to 45000 M^{-1} cm^{-1}. Compared with traditional rhodamine dyes,[7,16] the **AFR** dyes had larger Stokes shifts (>50 nm) in H_2O, which could reduce the level of self-absorption, help produce a high resolution, and facilitate multichannel bioimaging.[4b,17]

The pH stability of the **AFR** dyes was measured in different Britton-Robinson (BR) buffers (40 mM, pH 2−11). As seen in Figure 2 and Figure S3 of the Supporting Information, the absorption intensity of **AFR1** remains almost the same over a wide pH range (4.0−10.0). This result indicates wider pH stability for **AFR1** than for traditional rhodamine dyes,[7] which implies that the formation of spirolactone for **AFR1** is difficult probably because of the introduction of aminobenzofuran. **AFR1E** and **AFR2** showed the same tendency, and their

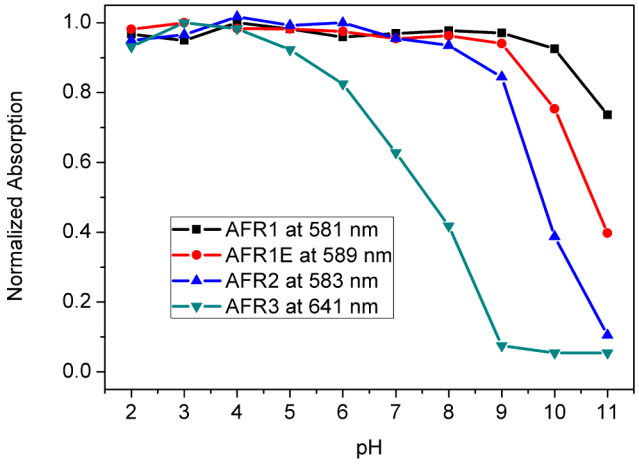

Figure 2. pH dependence of the normalized absorption of **AFR** dyes in BR buffers (40 mM, pH 2−11).

absorption intensity varied very little in the pH range of 2−9. **AFR3** had strong absorption intensity only under acidic conditions (from 2.0 to 6.0), but the intensity dropped between pH 6 and 11. Under alkaline environment conditions, the position directly connected with CF_3 of **AFR3** might be easily attached by hydroxyl, resulting in structural destruction. Nonetheless, it had little influence on the bioimaging properties of **AFR3** because of the location in the acid organelle (lysosome, pH 4.6−5.0)[18] in the cells.

Bioimaging and Cell Location. To further demonstrate the potential applications of **AFR** dyes in biological samples, we conducted fluorescent imaging cell location experiments in A549 cells. As shown in Figure 3, **AFR** dyes were easily

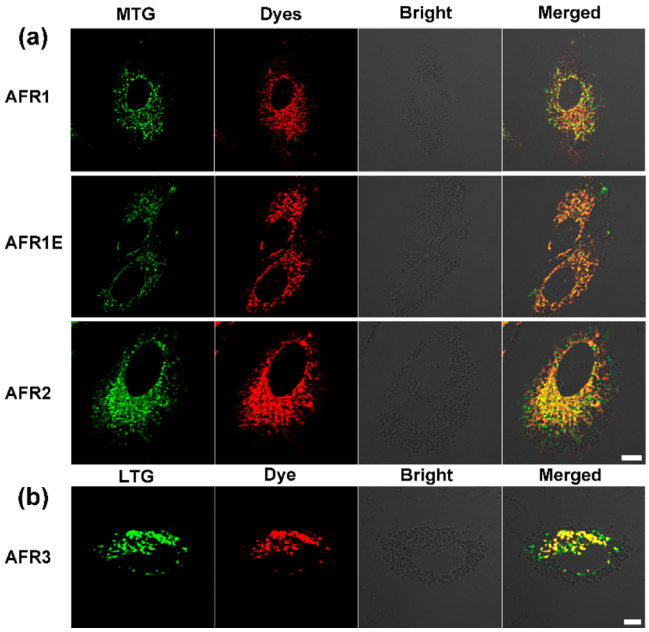

Figure 3. Confocal fluorescence microscopy images of A549 cells incubated with (a) MTG (100 nM) and compound **AFR1**, **AFR1E**, or **AFR2** (2 μM) and (b) LTG (200 nM) and compound **AFR3** (5 μM). The scale bar is 10 μm.

permeating the living cells at the optimal concentration, and obvious stains in the cytoplasm were observed. Generally, positively charged rhodamine derivatives are mainly located in the mitochondria by electrostatic interactions.[7b,19] Hence, MitoTracker Green FM (MTG) as the standard mitochondria marker was first used to confirm the localization of **AFR** dyes in the A549 cells. **AFR1**, **AFR1E**, and **AFR2** are mainly located in the mitochondria with 90−99% overlap with MTG (Figure 3a). As for **AFR3**, it had little overlap with MTG in A549 cells (data not shown), which properly stained lysosome. The colocalization experiment of **AFR3** with LysoTracker Green (LTG, a commercially available lysosome specific staining probe) demonstrated that fluorescence throughout the cytoplasm is predominantly associated with lysosomes (Figure 3b).

Photostability and Cytotoxicity. It is vital to note that evaluating the photostability of **AFR** dyes is crucial for imaging-related applications in living cells. The photostability of **AFR** dyes was evaluated in A549 cells by continuous irradiation (Figure 4). After irradiation for 20 min, the intensity of **AFR1** decreased to 95%, whereas those of **AFR1E** and **AFR2** decreased to 76 and 74%, respectively. However, as a comparison, the intensity of the MTG dropped to 12% in 20

DOI: 10.1021/acs.joc.5b00077
J. Org. Chem. 2015, 80, 3170−3175

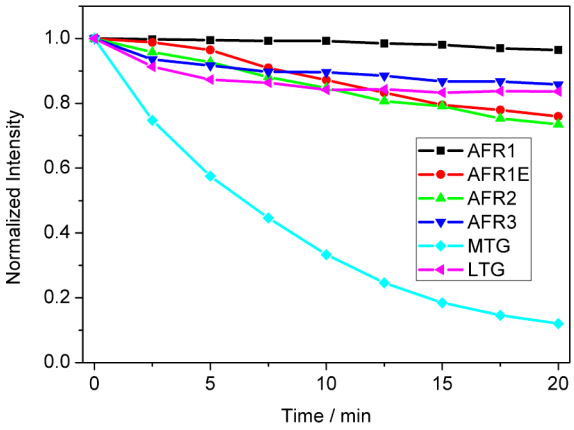

Figure 4. Photostability of **AFR** dyes, MTG, and LTG in A549 cells.

min. As for **AFR3**, more than 85% of the initial fluorescence intensity remained after irradiation for 20 min, which was roughly equal to that of LTG. The results mentioned above revealed that the **AFR** dyes had comparable photostability, which could be applied to long-term monitoring biological events in living samples.

The cytotoxicity of the **AFR** dyes in the A549 and HeLa cells was tested via MTT [3-(4,5-dimethylthiazol-2-yl)-2,5-diphenyl-2*H*-tetrazolium] assay. As seen in Figure 5, all the compounds

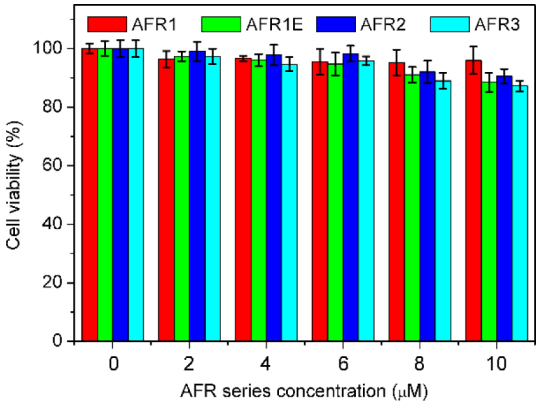

Figure 5. Cytotoxicity of **AFR** dyes in A549 cells.

exhibited very low cytotoxicity after incubation in A549 cells for 24 h even if the concentration was up to 10 μM. At this concentration, the cell viabilities of **AFR** dyes were >85%. The results of the MTT assay in HeLa cells (Figure S5 of the Supporting Information) are in good agreement with the results for A549 cells. These results indicate that the **AFR** dyes are biocompatible because of their low cytotoxicity in both A549 and HeLa cells.

CONCLUSIONS

In conclusion, a series of amino group-containing and benzofuran-fused rhodamine derivatives (**AFR1**, **AFR1E**, **AFR2**, and **AFR3**) with excellent photophysical properties and good biocompatibility were synthesized. **AFR1**, **AFR1E**, and **AFR2** show deep-red emission, high fluorescence quantum yield, good photostability, and a wide region of pH stability. To the best of our knowledge, NIR **AFR3** emits the longest fluorescence with comparable photostability among all the amino group-containing rhodamine derivatives. Data from cell imaging showed that **AFR1**, **AFR1E**, and **AFR2** are mainly located in the mitochondria, and **AFR3** is a lysosome tracker. Our work demonstrated an alternative strategy for obtaining a high quantum yield, a large Stokes shift, and long wavelength fluorescent dyes. Further studies using the **AFR** dyes for detection and imaging applications in biological samples are underway in our laboratory.

EXPERIMENTAL SECTION

Quantum Yield (QY) Measurement. Cresyl violet in methanol (Φ = 0.54) was chosen as the standard for measuring the quantum yield of **AFR1**, **AFR1E**, and **AFR2**.[20] As for the quantum yield of **AFR3**, zinc phthalocyanine in toluene (containing 1% pyridine; Φ = 0.30) was the standard.[21] The quantum yield of the **AFR** dyes in different solvents was calculated according to the equation $\Phi_x = \Phi_{st}(n_x^2/n_{st}^2)(G_x/G_{st})$, where Φ is the quantum yield, G is the gradient from the plot of integrated fluorescence intensity versus absorbance, n is the refractive index (n_{MeOH} = 1.329, $n_{CH_2Cl_2}$ = 1.424, n_{EtOH} = 1.361, n_{H_2O} = 1.333, and $n_{toluene}$ = 1.497), and A is the absorbance at the excitation wavelength (λ_{ex} = 540 nm for **AFR1**, **AFR1E**, and **AFR2**, λ_{ex} = 605 nm for **AFR3**). Subscripts x and st refer to the unknown and standard fluorophores, respectively. Related data are included in the Supporting Information (Figure S4 and Table S1).

Imaging. A human non-small cell lung cancer cell line (A549 cells) was used to perform all the imaging-related experiments (including the MTT assay), while a human uterine cervical cancer cell line (HeLa cells) was used only to evaluate the cytotoxicity of **AFR** dyes by the MTT assay. A549 and HeLa cells were cultured in confocal dishes in culture media [McCoy's 5A and Dulbecco's modified Eagle's medium (DMEM) respectively, supplemented with 10% fetal bovine serum (FBS), 50 units/mL penicillin, and 50 mg/mL streptomycin] under a 5% CO_2/air atmosphere at 37 °C in a humidified incubator for 24 h. Then 2 or 5 μL of the **AFR** dye solution (stock solution, 1 mM in DMSO) was added to the culture medium of A549 cells and incubated at 37 °C under 5% CO_2 for 30 min before being imaged. (For colocalization experiments, A549 cells were treated and incubated with 100 nM MTG or 200 nM LTG.) Cells were washed with PBS (pH 7.4) three times before being imaged. Images were aquired with a Nikon C1si laser scanning confocal microscope (excitation at 488 nm, FITC channel; excitation at 543 nm, TRITC channel; excitation at 640 nm, DAPI channel) and processed with NIS-Elements Viewer 3.20. For photostability, **AFR1**, **AFR1E**, **AFR2**, MTG, and LTG were continuously irradiated with a 488 nm laser, and a 640 nm laser was used for **AFR3**.

MTT Assay. **AFR** dye stock solutions (1 mM each) were diluted with fresh medium (McCoy's 5A and DMEM were utilized for A549 and HeLa cells, respectively) to different concentrations (0, 2, 4, 6, 8, and 10 μM). A549 or HeLa cells were cultured in a 96-well plate for 12 h, and then the cell medium was exchanged with different concentrations of **AFR** solutions, which were removed after incubation for 2 h and exchanged with fresh medium. After a 24 h incubation at 37 °C in 5% CO_2, the cell medium were exchanged with fresh medium (100 μL), and then 20 μL of the MTT (5 mg/mL) solution was added to each well. After incubation at 37 °C in 5% CO_2 for 4 h, 100 μL of DMSO was added after the culture medium had been discarded. The absorbance for all the wells with cell medium was measured at 570 nm, and the cell viability of untreated cells was set to 100% as a reference.

Synthesis of *N*-(3-Methoxyphenyl)acetamide (2). The published method was followed to synthesize compound **2**.[22] Acetic anhydride (20 mL) was added to a solution of *m*-anisidine (20 g, 16.25 mmol) in 20 mL of acetic acid at 0 °C. The solution was stirred for 24 h at room temperature and then poured into the mixture of 100 g of ice and 100 mL of water. The light pink solid was filtered and dried under vacuum, yielding 15.6 g (58%) of the product. ^{1}H NMR (400 MHz, DMSO-d_6): δ 9.89 (s, 1H), 7.28 (t, 1H, J = 2.1 Hz), 7.18 (t, 1H, J = 8.1 Hz), 7.10 (d, 1H, J = 8.5 Hz), 6.62–6.58 (m, 1H), 3.71 (s, 3H), 2.03 (s, 3H). ^{13}C NMR (100 MHz, DMSO-d_6): δ 168.3, 159.5, 140.5,

DOI: 10.1021/acs.joc.5b00077
J. Org. Chem. 2015, 80, 3170−3175

129.4, 111.3, 108.3, 104.9, 54.9, 24.1. TOF-EI calcd for $[C_9H_{11}NO_2]$ m/z 165.0789, found m/z 165.0743.

Synthesis of *N*-(3-Oxo-2,3-dihydrobenzofuran-6-yl)-acetamide (3). A modified method was followed to synthesize compound **3**.[12] Chloroacetyl chloride (6.52 g, 58.2 mmol) was added, followed within 15 min by 4 g (24.2 mmol) of *N*-(3-methoxyphenyl)-acetamide, to a solution of 12.92 g (98.0 mmol) of $AlCl_3$ in 20 mL of 1,2-dichloroethane at 0 °C under N_2. The mixture was stirred for 30 min at 0 °C, slowly warmed to room temperature, and further stirred for 24 h. The brown mixture was added to 200 mL of ice−water and 200 mL of AcOEt. After the mixture had been vigorously stirred, the resulting precipitate [*N*-(3-methoxy-4-chloroacetylphenyl)acetamide] was filtered off and dried under vacuum. The resulting solid was introduced into 30 mL of EtOH; 2.64 g (32.2 mmol) of AcONa was added, and then the mixture was heated under reflux for 24 h. EtOH was removed under reduced pressure, and the mixture solid was purified by silica gel chromatography using a 1:2 (v/v) petroleum ether/AcOEt mixture as the eluent to give **3** as a yellow solid (1.47 g, 32%). ^{1}H NMR (400 MHz, DMSO-d_6): δ 10.45 (s, 1H), 7.71 (d, 1H, J = 1.4 Hz), 7.56 (d, 1H, J = 8.4 Hz), 7.14 (dd, 1H, J_1 = 8.5 Hz, J_2 = 1.6 Hz), 4.75 (s, 2H), 2.11 (s, 3H). ^{13}C NMR (100 MHz, DMSO-d_6): δ 197.5, 174.5, 169.4, 147.9, 124.2, 115.6, 113.4, 101.5, 75.2, 24.3. TOF-EI calcd for $[C_{10}H_9NO_3]$ m/z 191.0582, found m/z 191.0534.

Synthesis of 3-(Diethylamino)phenyl Acetate (5). Ac_2O (765 μL, 8 mmol), DMAP (31 mg, 0.25 mmol), and NEt_3 (845 μL, 6 mmol) were successively added to an anhydrous CH_2Cl_2 (10 mL) solution of 3-(diethylamino)phenol (852 mg, 5 mmol), which was stirred for 12 h. The mixture solution was extracted with 100 mL of CH_2Cl_2. The organic layer was washed with a saturated $NaHCO_3$ (2 × 30 mL) solution and brine (2 × 30 mL) and dried with anhydrous $MgSO_4$. After being dried, CH_2Cl_2 was removed under reduced pressure, and the final solution was purified by silica gel chromatography using an 8:1 (v/v) petroleum ether/AcOEt mixture as the eluent to give **5** as a light yellow oily liquid (1.02 g, 98%). ^{1}H NMR (400 MHz, $CDCl_3$): δ 7.17 (t, 1H, J = 8.0 Hz), 6.54−6.48 (m, 1H), 6.34 (d, 2H, J = 7.5 Hz), 3.32 (q, 4H, J = 7.1 Hz), 2.28 (s, 3H), 1.15 (t, 6H, J = 7.1 Hz). ^{13}C NMR (100 MHz, $CDCl_3$): δ 170.6, 153.0, 150.0, 130.7, 110.1, 108.9, 105.6, 45.3, 22.2, 13.4. TOF-EI calcd for $[C_{12}H_{17}NO_2]$ m/z 207.1259, found m/z 207.1293.

Synthesis of 4-(Dimethylamino)-1′,1′,1′-trifluoro-2-hydroxyacetophenone (6). A modified method was followed to synthesize compound **6**.[14] A solution of **5** (2.04 g, 9.86 mmol) and trifluoroacetic anhydide (3.45 mL, 24.6 mmol) in Et_2O (20 mL) was refluxed for 3 h, and the solvent was evaporated. The residue, dissolved in a mixture of THF (40 mL) and 2 M aqueous hydrochloric acid (20 mL), was stirred for 24 h at room temperature. The solution was concentrated under reduced pressure, and the aqueous residue was extracted with ether. The organic extract was washed with water and brine, dried, and evaporated. The residue was crystallized (petroleum ether) to give **4** as yellow needles (1.03 g, 40%). ^{1}H NMR (400 MHz, $CDCl_3$): δ 11.83 (s, 1H), 7.57 (dq, 1H, J_1 = 9.4 Hz, J_2 = 2.1 Hz), 6.27 (dd, 1H, J_1 = 9.5 Hz, J_2 = 2.6 Hz), 6.11 (d, 1H, J = 2.6 Hz), 3.44 (q, 4H, J = 7.1 Hz), 1.23 (t, 6H, J = 7.1 Hz). ^{13}C NMR (100 MHz, $CDCl_3$): δ 180.2 (q, J = 34 Hz), 168.2, 156.1, 133.3 (q, J = 4 Hz), 118.3 (q, J = 287 Hz), 106.3, 105.2, 98.0, 45.9, 13.5 (F atom effect-induced split of ^{13}C NMR).[23] ^{19}F NMR (376 MHz, DMSO-d_6): δ −68.6 (s, 3F). TOF-EI calcd for $[C_{12}H_{14}F_3NO_2]$ m/z 261.0977, found m/z 261.0950.

Synthesis of AFR1. Compound **3** (382 mg, 2.0 mmol) and compound **7** (640 mg, 2.0 mmol) were successively added to concentrated H_2SO_4 (10 mL), which was heated at 100 °C for 4 h. After being cooled, the mixture was poured into ice−water, and then perchloric acid (2 mL) was added. The resulting precipitate was filtered off and washed with plenty of water. After the sample had dried, purification by silica gel chromatography using a CH_2Cl_2/CH_3OH mixture [20:1, 10:1, 5:1, or 3:1 (v/v)] as the eluent gave **AFR1** as a dark-blue solid (945 mg, 90%). Mp: 292−294 °C. ^{1}H NMR (400 MHz, DMSO-d_6): δ 13.22 (s, 1H), 8.16 (d, 1H, J = 7.5 Hz), 7.86 (t, 1H, J = 7.4 Hz), 7.83−7.74 (m, 2H), 7.52 (d, 1H, J = 7.2 Hz), 7.28−6.78 (m, 6H), 6.65 (s, 1H), 3.53 (q, 4H, J = 6.7 Hz), 1.17 (t, 6H, J = 7.0 Hz). ^{13}C NMR (100 MHz, CD_3OD): δ 166.0, 160.1, 158.5, 157.9, 155.8, 154.4, 142.1, 132.2, 132.0, 131.6, 131.3, 130.8, 124.8, 117.5, 115.7, 113.8, 106.4, 98.4, 94.8, 46.4, 12.7. ESI-HRMS calcd for $[C_{26}H_{23}N_2O_4]^+$ m/z 427.16523, found m/z 427.16504. Elem. Anal. Calcd for $C_{26}H_{23}ClN_2O_8$: C, 59.26; H, 4.40; N, 5.32. Found: C, 59.12; H, 4.53; N, 5.29.

Synthesis of AFR1E. Concentrated H_2SO_4 (2 mL) was added to an ethanol solution (10 mL) of compound **AFR1** (527 mg, 1.0 mmol), and the solution was heated to reflux for 4 h. After the sample had cooled, ethanol was removed under reduced pressure and the residue was slowly diluted with 50 mL of H_2O followed by 2 mL of $HClO_4$, which was stirred to collect the resulting precipitate. After the sample had dried, purification by silica gel chromatography using a CH_2Cl_2/CH_3OH [100:1, 80:1, or 60:1 (v/v)] as the eluent gave **AFR1E** as a dark-green solid (280 mg, 50%). Mp: 275−277 °C. ^{1}H NMR (400 MHz, DMSO-d_6): δ 8.26−8.22 (m, 1H), 7.96−7.92 (m, 2H), 7.86 (td, 1H, J_1 = 7.7 Hz, J_2 = 1.2 Hz), 7.80 (s, 2H), 7.65 (d, 1H, J = 6.7 Hz), 7.28 (d, 1H, J = 2.3 Hz), 7.25 (d, 1H, J = 9.4 Hz), 7.18 (dd, 1H, J_1 = 9.4 Hz, J_2 = 2.3 Hz), 6.97 (dd, 1H, J_1 = 9.0 Hz, J_2 = 1.6 Hz), 6.69 (d, 1H, J = 1.6 Hz), 4.03 (q, 2H, J = 7.1 Hz), 3.61 (q, 4H, J = 7.0 Hz), 1.20 (t, 6H, J = 7.0 Hz), 0.93 (t, 3H, J = 7.1 Hz). ^{13}C NMR (100 MHz, DMSO-d_6): δ 165.3, 164.1, 159.1, 155.9, 154.0, 152.6, 140.4, 139.3, 133.4, 131.3, 131.2, 130.4, 129.4, 129.0, 124.5, 117.2, 115.0, 111.7, 104.4, 97.5, 93.6, 61.5, 45.1, 13.7, 12.5. ESI-HRMS calcd for $[C_{28}H_{27}N_2O_4]^+$ m/z 455.19653, found m/z 455.19629. Elem. Anal. Calcd for $C_{28}H_{27}ClN_2O_8$: C, 60.60; H, 4.90; N, 5.05. Found: C, 60.71; H, 5.12; N, 5.09.

Synthesis of AFR2. Compound **3** (382 mg, 2.0 mmol) and compound **8** (394 mg, 2.0 mmol) were successively added to concentrated H_2SO_4 (10 mL), which was heated at 100 °C for 4 h. After being cooled, the mixture was poured into ice−water, and then perchloric acid (2 mL) was added. The resulting precipitate was filtered off and washed with plenty of water. After the sample had dried, purification by silica gel chromatography using a CH_2Cl_2/CH_3OH mixture [80:1, 60:1, 40:1, or 20:1 (v/v)] as the eluent gave **AFR2** as a dark-blue solid (560 mg, 69%). Mp: 254−256 °C. ^{1}H NMR (400 MHz, DMSO-d_6): δ 8.69 (d, J = 16.5 Hz, 1H), 7.95−7.83 (m, 2H), 7.77 (s, 2H), 7.26 (d, J = 8.9 Hz, 1H), 7.16 (s, 1H), 6.94 (d, J = 8.9 Hz, 1H), 6.76 (s, 1H), 3.60 (q, J = 6.2 Hz, 4H), 1.20 (t, J = 7.0 Hz, 6H). ^{13}C NMR (100 MHz, 2:1 CD_3OD/CD_2Cl_2): δ 166.1, 160.2, 157.0, 156.4, 154.2, 143.6, 132.5, 126.4, 124.6, 117.7, 115.4, 113.4, 105.5, 97.8, 94.3, 46.1, 12.3. ESI-HRMS calcd for $[C_{19}H_{19}N_2O_2]^+$ m/z 307.14410, found m/z 307.144409. Elem. Anal. Calcd for $C_{19}H_{19}ClN_2O_6$: C, 56.09; H, 4.71; N, 6.89. Found: C, 55.91; H, 4.78; N, 6.91.

Synthesis of AFR3. Compound **3** (382 mg, 2.0 mmol) and compound **6** (522 mg, 2.0 mmol) were successively added to concentrated H_2SO_4 (10 mL), which was heated at 100 °C for 8 h. After being cooled, the mixture was poured into ice−water, and then perchloric acid (2 mL) was added. The resulting precipitate was filtered off and washed with plenty of water. After the sample had dried, purification by silica gel chromatography using a CH_2Cl_2/CH_3OH mixture [200:1, 150:1, 100:1, or 80:1 (v/v)] as the eluent gave **AFR3** as a green solid (105 mg, 11%). Mp: 265−268 °C. ^{1}H NMR (400 MHz, DMSO-d_6): δ 8.60 (s, 2H), 7.94 (dd, 1H, J_1 = 9.0 Hz, J_2 = 1.9 Hz), 7.81 (d, 1H, J = 9.4 Hz), 7.29 (d, 1H, J = 9.5 Hz), 7.22 (s, 1H), 7.01 (d, 1H, J = 9.0 Hz), 6.82 (s, 1H), 3.61 (q, 4H, J = 6.9 Hz), 1.20 (t, 6H, J = 7.0 Hz). ^{13}C NMR (100 MHz, DMSO-d_6): δ 165.8, 161.8, 156.8, 155.5, 152.1, 140.9, 127.0, 126.0, 121.8 (d, J = 275 Hz), 118.9, 118.2 (d, J = 35 Hz), 115.3, 106.2, 104.9, 98.3, 94.3, 45.3, 12.8 (F atom effect-induced split of ^{13}C NMR).[23] ^{19}F NMR (376 MHz, DMSO-d_6): δ −56.4 (s, 3F). ESI-HRMS calcd for $[C_{20}H_{18}F_3N_2O_2]^+$ m/z 375.13149, found m/z 375.13133. Elem. Anal. Calcd for $C_{20}H_{18}ClF_3N_2O_6 \cdot {}^1/_4H_2O$: C, 50.12; H, 3.89; N, 5.84. Found: C, 50.09; H, 3.91; N, 5.82.

DOI: 10.1021/acs.joc.5b00077
J. Org. Chem. 2015, 80, 3170−3175

■ ASSOCIATED CONTENT

Supporting Information

Photophysical data, cell data, and NMR spectra of new compounds. This material is available free of charge via the Internet at http://pubs.acs.org.

■ AUTHOR INFORMATION

Corresponding Author

*E-mail: wmliu@mail.ipc.ac.cn.

Notes

The authors declare no competing financial interest.

■ ACKNOWLEDGMENTS

This work was supported by the NNSF of China (Grants 21373250, 21173244, and F040801).

■ REFERENCES

(1) (a) Kobayashi, H.; Ogawa, M.; Alford, R.; Choyke, P. L.; Urano, Y. *Chem. Rev.* **2010**, *110*, 2620. (b) Chen, X.; Pradhan, T.; Wang, F.; Kim, J. S.; Yoon, J. *Chem. Rev.* **2012**, *112*, 1910. (c) Chan, J.; Dodani, S. C.; Chang, C. J. *Nat. Chem.* **2012**, *4*, 973. (d) Li, X.; Gao, X.; Shi, W.; Ma, H. *Chem. Rev.* **2014**, *114*, 590.

(2) (a) Fan, J.; Hu, M.; Zhan, P.; Peng, X. *Chem. Soc. Rev.* **2013**, *42*, 29. (b) Zheng, H.; Zhan, X.-Q.; Bian, Q.-N.; Zhang, X.-J. *Chem. Commun.* **2013**, *49*, 429.

(3) (a) Lippert, A. R.; New, E. J.; Chang, C. J. *J. Am. Chem. Soc.* **2011**, *133*, 10078. (b) Lin, V. S.; Lippert, A. R.; Chang, C. J. *Proc. Natl. Acad. Sci. U.S.A.* **2013**, *110*, 7131. (c) Sakabe, M.; Asanuma, D.; Kamiya, M.; Iwatate, R. J.; Hanaoka, K.; Terai, T.; Nagano, T.; Urano, Y. *J. Am. Chem. Soc.* **2013**, *135*, 409. (d) Komatsu, T.; Hanaoka, K.; Adibekian, A.; Yoshioka, K.; Terai, T.; Ueno, T.; Kawaguchi, M.; Cravatt, B. F.; Nagano, T. *J. Am. Chem. Soc.* **2013**, *135*, 6002.

(4) (a) Weissleder, R. *Nat. Biotechnol.* **2001**, *19*, 316. (b) Escobedo, J. O.; Rusin, O.; Lim, S.; Strongin, R. M. *Curr. Opin. Chem. Biol.* **2010**, *14*, 64. (c) Yuan, L.; Lin, W.; Zheng, K.; He, L.; Huang, W. *Chem. Soc. Rev.* **2013**, *42*, 622.

(5) (a) Fu, M. Y.; Xiao, Y.; Qian, X. H.; Zhao, D. F.; Xu, Y. F. *Chem. Commun.* **2008**, 1780. (b) Koide, Y.; Urano, Y.; Hanaoka, K.; Terai, T.; Nagano, T. *J. Am. Chem. Soc.* **2011**, *133*, 5680. (c) Koide, Y.; Urano, Y.; Hanaoka, K.; Terai, T.; Nagano, T. *ACS Chem. Biol.* **2011**, *6*, 600.

(6) (a) Kushida, Y.; Hanaoka, K.; Komatsu, T.; Terai, T.; Ueno, T.; Yoshida, K.; Uchiyama, M.; Nagano, T. *Bioorg. Med. Chem. Lett.* **2012**, *22*, 3908. (b) Piao, W.; Tsuda, S.; Tanaka, Y.; Maeda, S.; Liu, F.; Takahashi, S.; Kushida, Y.; Komatsu, T.; Ueno, T.; Terai, T.; Nakazawa, T.; Uchiyama, M.; Morokuma, K.; Nagano, T.; Hanaoka, K. *Angew. Chem., Int. Ed.* **2013**, *52*, 13028.

(7) Furukawa, K.; Abe, H.; Wang, J.; Uda, M.; Koshino, H.; Tsuneda, S.; Ito, Y. *Org. Biomol. Chem.* **2009**, *7*, 671.

(8) (a) Yuan, L.; Lin, W.; Yang, Y.; Chen, H. *J. Am. Chem. Soc.* **2012**, *134*, 1200. (b) Chen, J.; Liu, W.; Zhou, B.; Niu, G.; Zhang, H.; Wu, J.; Wang, Y.; Ju, W.; Wang, P. *J. Org. Chem.* **2013**, *78*, 6121. (c) Liu, J.; Sun, Y.-Q.; Wang, P.; Zhang, J.; Guo, W. *Analyst* **2013**, *138*, 2654. (d) Kamino, S.; Murakami, M.; Tanioka, M.; Shirasaki, Y.; Watanabe, K.; Horigome, J.; Ooyama, Y.; Enomoto, S. *Org. Lett.* **2014**, *16*, 258.

(9) (a) Haley, L. N. F. *J. Heterocycl. Chem.* **1977**, *14*, 683. (b) Shi, J. M.; Zhang, X. P.; Neckers, D. C. *Tetrahedron Lett.* **1993**, *34*, 6013. (c) Sauer, M.; Han, K. T.; Mueller, R.; Schulz, A.; Tadday, R.; Seeger, S.; Wolfrum, J.; Arden-Jacob, J.; Deltau, G.; Marx, N. J.; Drexhage, K. H. *J. Fluoresc.* **1993**, *3*, 131.

(10) (a) Ustinov, A.; Korshun, V. US 20120316319 A1, 2012. (b) Pastierik, T.; Šebej, P.; Medalová, J.; Štacko, P.; Klán, P. *J. Org. Chem.* **2014**, *79*, 3374.

(11) (a) Umezawa, K.; Nakamura, Y.; Makino, H.; Citterio, D.; Suzuki, K. *J. Am. Chem. Soc.* **2008**, *130*, 1550. (b) Son, J. H.; Lim, C. S.; Han, J. H.; Danish, I. A.; Kim, H. M.; Cho, B. R. *J. Org. Chem.* **2011**, *76*, 8113. (c) Chen, J.; Liu, W.; Ma, J.; Xu, H.; Wu, J.; Tang, X.; Fan, Z.; Wang, P. *J. Org. Chem.* **2012**, *77*, 3475. (d) Bochkov, A. Y.; Akchurin, I. O.; Dyachenko, O. A.; Traven, V. F. *Chem. Commun.* **2013**, *49*, 11653.

(12) Diedrichs, N.; Fahrig, T.; Gerlach, I.; Ragot, J.; Schuhmacher, J.; Thede, K.; Horvath, E. WO 2005113529 A2, 2005.

(13) Anzalone, A. V.; Wang, T. Y.; Chen, Z. X.; Cornish, V. W. *Angew. Chem., Int. Ed.* **2013**, *52*, 650.

(14) Corrie, J. E. T.; Munasinghe, V. R. N.; Rettig, W. *J. Heterocycl. Chem.* **2000**, *37*, 1447.

(15) Sommer, J. R.; Shelton, A. H.; Parthasarathy, A.; Ghiviriga, I.; Reynolds, J. R.; Schanze, K. S. *Chem. Mater.* **2011**, *23*, 5296.

(16) (a) Sreenath, K.; Clark, R. J.; Zhu, L. *J. Org. Chem.* **2012**, *77*, 8268. (b) Cui, X.; Zhao, J.; Lou, Z.; Li, S.; Wu, H.; Han, K.-l. *J. Org. Chem.* **2015**, *80*, 568.

(17) Lakowicz, J. R. *Principles of fluorescence spectroscopy*, 2nd ed.; Kluwer Academic: New York, 1999.

(18) Luzio, J. P.; Pryor, P. R.; Bright, N. A. *Nat. Rev. Mol. Cell Biol.* **2007**, *8*, 622.

(19) (a) Johnson, L. V.; Walsh, M. L.; Chen, L. B. *Proc. Natl. Acad. Sci. U.S.A.* **1980**, *77*, 990. (b) Koide, Y.; Urano, Y.; Kenmoku, S.; Kojima, H.; Nagano, T. *J. Am. Chem. Soc.* **2007**, *129*, 10324. (c) Kim, Y. K.; Ha, H. H.; Lee, J. S.; Bi, X. Z.; Ahn, Y. H.; Hajar, S.; Lee, J. J.; Chang, Y. T. *J. Am. Chem. Soc.* **2010**, *132*, 576.

(20) Magde, D.; Brannon, J. H.; Cremers, T. L.; Olmsted, J. *J. Phys. Chem.* **1979**, *83*, 696.

(21) Vincett, P. S.; Voigt, E. M.; Rieckhoff, K. E. *J. Chem. Phys.* **1971**, *55*, 4131.

(22) Akhavan-Tafti, H.; DeSilva, R.; Arghavani, Z.; Eickholt, R. A.; Handley, R. S.; Schoenfelner, B. A.; Sugioka, K.; Sugioka, Y.; Schaap, A. P. *J. Org. Chem.* **1998**, *63*, 930.

(23) Dolbier, W. R. *Guide to fluorine NMR for organic chemists*; John Wiley & Sons: New York, 2009.

DOI: 10.1021/acs.joc.5b00077
J. Org. Chem. 2015, 80, 3170−3175